Superradiant Light Scattering from Thermal Atomic Vapors

Yutaka Yoshikawa,* Yoshio Torii, and Takahiro Kuga

Institute of Physics, University of Tokyo, 3-8-1, Meguro-ku, Komaba, Tokyo 153-8902, Japan.

(Received 12 July 2004; published 4 March 2005)

Superradiant light scattering from noncondensed, thermal atomic vapors was experimentally studied. We found that superradiant gain is independent of quantum degeneracy and determined only by the shape of the atomic cloud and a contained number of atoms. Superradiant pump-probe spectroscopy was also developed to measure the atomic correlation function, revealing the Doppler-width-limited coherence time of the thermal gas and sudden buildup of long-lived coherence below the transition temperature.

DOI: 10.1103/PhysRevLett.94.083602 PACS numbers: 42.50.Gy, 03.75.–b, 32.80.–t

After the realization of Bose-Einstein condensation of dilute gas, collective light scattering from condensates, referred to as superradiant light scattering (SLS), has attracted considerable attention [1–6]. This phenomenon was regarded as a four-wave mixing between light and matter waves [5], and developed to the demonstration of coherent matter-wave amplification [7]. These experiments have pioneered a new research field of coherent atom optics; however, there is still a fundamental question of whether the similar phenomenon would be observable in noncondensed and fermionic atoms. While several authors predicted that SLS occurs for such samples if its gain exceeds the decoherence of the system [8,9], no experimental demonstration has been reported so far, and it was attributed to the low gain and short coherence time-of momentum-spread atoms [1,9].

In this Letter, we report on the first observation of SLS from evaporatively cooled, thermal rubidium (Rb) vapors. We studied the gain properties of SLS both above and below the phase transition temperature T_c to find, contrary to the previous argument, less dependence on the atomic temperature. We also performed superradiant pump-probe spectroscopy to measure the correlation function of atoms, identifying significant difference in coherence time between thermal and condensate component.

The experimental procedure is similar to that of our previous work [3]. Briefly, a cigar-shaped cloud of evaporatively cooled ^{87}Rb atoms in the state $|2\rangle \equiv |5S_{1/2}; F = 2, m_F = 2\rangle$ was illuminated by a single, off-resonant pump beam as shown in Fig. 1(a). The light wavelength λ was 795 nm (tuned around the D_1 line), and the polarization was set to be parallel to the long axis of the cloud, which is equal to the quantization axis of the magnetic sublevels (defined as z axis). This π-polarized pump beam induces the Raman-type SLS that transfers the atoms into the state $|1\rangle \equiv |5S_{1/2}; F = 1, m_F = 1\rangle$ [10]. Raman photons are emitted mainly along the z direction (so-called "end-fire" mode), due to the anisotropic gain of a cigar-shaped atomic cloud [1,5]. The transferred atoms into the state $|1\rangle$ thus received a photon-recoil momentum $\hbar q = \sqrt{2}h/\lambda = \sqrt{2}\hbar k$ along the direction of unit vectors $(\hat{\boldsymbol{x}} \pm \hat{\boldsymbol{z}})/\sqrt{2}$.

In the Raman-type SLS, position- and state-dependent energy shift, such as inhomogeneous Zeeman shift, causes much shorter coherence time than that of the Rayleigh-type SLS [2]. Hence, in the present work, we applied the pump beam after turning off the magnetic trap. Instead, a homogeneous magnetic field of ~0.3 G was applied along the z direction to prevent unexpected spin flips. The atomic velocity distribution was analyzed by state-selective absorption imaging [3] along the y direction. In addition, to monitor the evolution of SLS, one of the end-fire modes was collected by two lenses of NA (numerical aperture) = 0.19 and detected with a photo-multiplier tube (PMT).

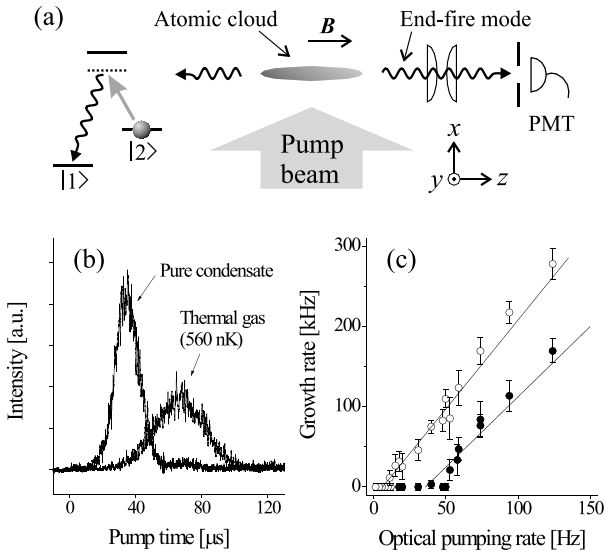

FIG. 1. (a) Schematic diagram of the experiment. Emitted superradiant Raman photons were collected by lenses and impinged upon a photo-multiplier tube (PMT). (b) Observed waveform of the end-fire mode emitted from a nearly pure condensate (faster pulse) and noncondensed gas of $T = 560$ nK (slower pulse) for a single-atom optical pumping rate $R = 75$ Hz. Exponential growth rate obtained by initial rise of these signals is plotted vs R in (c). Open and closed circles correspond to the condensate and the thermal gas of $T = 560$ nK, respectively. Solid lines are linear fits to the data.

Figure 1(b) shows typical pulse shapes emitted from a nearly pure condensate and a thermal gas of $T = 560$ nK (in our setup, $T_c = 519(9)$ nK). The detuning from the excited state δ and the pump-beam intensity I was $2\pi \times -2.6$ GHz and 180 mW/cm^2, respectively, and the corresponding single-atom optical pumping rate R was 75 Hz. We note that increasing R around 400 Hz gives a similar signal even for much hotter atoms up to $\sim 3\ \mu$K. Furthermore, we were also able to observe the Rayleigh-type SLS [1], triggered by a y-polarized pump beam [11], for a similar temperature range.

As can be seen in Fig. 1(b), the signal from the thermal gas indicated a slower initial rise compared to that from the condensate. We fitted these rises with an exponential growth function and plotted the obtained growth rate versus R in Fig. 1(c). Open and closed circles correspond to the pure condensate and the thermal gas, respectively. The existence of a ''threshold'' and linear dependence of the growth rate on R is a common feature to both samples [1]. The slope of the data represents the gain factor of SLS given as $g \simeq 3\lambda^2 N_2/(2\pi A)$, with A being the cross section of the atomic cloud in the x-y plane and N_i the total number of atoms in the state $|i\rangle$ ($i = 1, 2$). Notice that both A and N_2 of evaporatively cooled atoms are generally larger for higher temperatures. As a result, the dependence of g on T is weak, and g is still on the same order even for $T > T_c$. In fact, g for the condensate and the thermal gas of 560 nK is predicted to be 3500 ($A = 120\ \mu$m^2, $N_2 = 1.4 \times 10^6$ atoms) and 3200 ($A = 1040\ \mu$m^2, $N_2 = 11 \times 10^6$ atoms), respectively. For Fig. 1(c), linear fit to the data gives $g = 2240$ for the condensate and 1760 for the thermal gas. Thus, one can see a small difference within a factor of 2, probably due to localization of the SLS process (discussed later). However, their ratio 0.79 shows fairly well agreement with the theoretical value 0.91. This means that g is indeed scaled as N_2/A and independent of whether the atoms are condensed.

In the wave mixing of momentum-spread atoms, the initial momentum width Δp must be preserved in the recoiling state because of momentum conservation [9,12]. To verify this point, we compared the atomic velocity distribution before and after the light scattering. Figures 2(a) and 2(b) show time-of-flight images of the initial atoms in the state $|2\rangle$ and recoiling atoms pumped into the state $|1\rangle$, respectively. Their cross sections along the x direction are plotted in Fig. 2(c). Here, by degrading efficiency of evaporative cooling, we specially prepared a pure thermal gas of 473(7) nK. The image of the state $|2\rangle$ was taken with an off-resonant probe laser to effectively reduce the optical density by a factor of 2.

The distribution of the recoiling atoms was similar to that of the initial atoms, except for a center-of-mass displacement and a slight long tail at the left side. The displacement represents a translational velocity 5.60 mm/s, in good agreement with the x component of the recoil velocity 5.75 mm/s. Although the asymmetric distribution is a bit troublesome to determine the temperature, here we

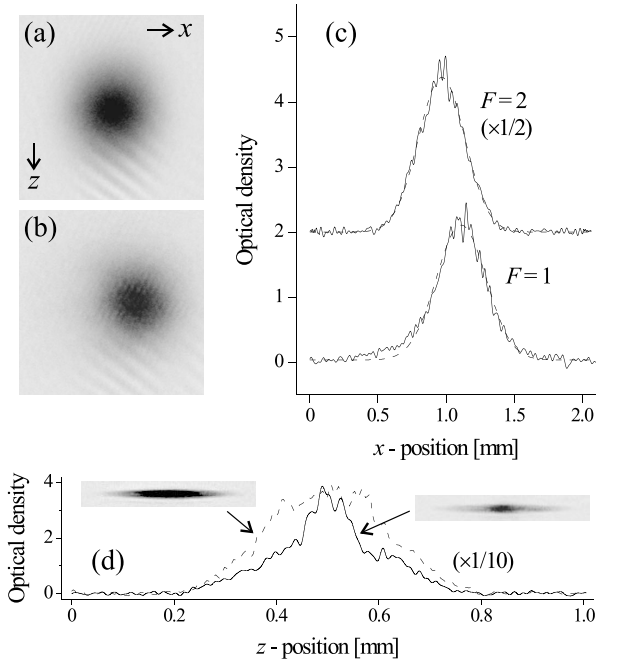

FIG. 2. Absorption images after 25-ms time of flight for (a) the original $F = 2$ atoms and (b) the recoiling $F = 1$ atoms. Field of view is 1.2 mm × 1.2 mm. Cross sections of these density distributions along the x direction are compared in (c). The data on the $F = 2$ atoms were added by an offset of 2 for clarity. Dashed lines are Gaussian fitting, leading to the temperature of 473(7) nK for the $F = 2$ atoms and 544(11) nK for the $F = 1$ atoms. (d) 10-times reduced optical density of the preexpanding $F = 2$ cloud ($T \approx 650$ nK). Dashed (solid) line represents the atoms before (after) the SLS.

fitted it with a normal Gaussian function for simplicity. The resulting temperature 544(11) nK indicates heating of only about 70 nK, which is extremely smaller than that accompanied with spontaneous light scattering (on the order of 1 μK). We note that, in the time-of-flight image, two momentum side modes separated by $2\hbar k\hat{z}$ could not be distinguished. The main reason is simply the lack of momentum resolution, which is inevitable for atoms hotter than the recoil-limited temperature 349 nK (the momentum along the x direction can be highly resolved by state selectivity of the imaging).

When we took an image of ''preexpanding'' density distribution in the state $|2\rangle$, remarkable depletion at its shoulders was found after the light scattering [Fig. 2(d)]. It may be a result of local stimulated Raman scattering accompanied with propagation of the end-fire mode [13]. A similar phenomenon has been observed in the short-pulse superradiance [4]. Such localization reduces the number of atoms N_2 effectively and, accordingly, the net gain g.

In the previous works [8,9], SLS was discussed in terms of the atomic stimulation picture under the assumption of $\Delta p \ll \hbar q$. Then, a matter-wave grating is formed by two atomic motional states (polarization grating for Raman superradiance [2]) and stimulates the light scattering by

diffracting pump photons into the end-fire mode. Therefore, requirement for SLS was only the formation of a grating. In contrast, the present experiment was carried out in the regime $\Delta p > \hbar q$, where the thermal de Broglie length $h/\Delta p$ is smaller than the expected grating wavelength $2\pi/q$. This condition does not guarantee the formation of high-quality grating, and thus, the conventional picture of SLS mentioned above is inadequate.

However, if not the grating, the atomic coherence still plays an important role in the stimulated Raman process of SLS. In practice, it is the coherence time that is only the major difference between thermal gas and condensate. The simplest way to estimate the coherence time would be to determine the threshold of SLS [see Fig. 1(c)], since the stimulation is balanced with the decoherence at this moment [1]. Alternatively, here we performed pump-probe spectroscopy using SLS to study the coherence properties of the samples, involving classification of the decay line shape and measurement of multiple decoherence in partially condensed cloud.

Figure 3(a) shows an example of the timing sequence and acquired PMT signal. When the scattered light intensity reached its maximum, we turned off the pump beam at once, and, after a variable time, turned it on again as a "probe" of the atomic coherence (lower trace). The resulting PMT signal was split into two parts with different peak heights (upper trace). The ratio of these heights represents the remaining fraction of the coherence produced by the first pump-beam pulse. A similar technique was also employed for the measurement of subrecoil atomic temperature [14], and for the demonstration of matter-wave Raman amplifier [2].

To be more quantitative, we introduce the one-dimensional atomic wave function in the state $|i\rangle$ as $\Psi_i(p)$, where p represents the momentum along the photon-recoil direction. Neglecting the interatomic interaction, this is explicitly written as $\Psi_i(p) = \phi_i(p)e^{-i[\omega_i + p^2/(2m\hbar)]t}$, where $\phi_i(p)$ is the momentum distribution, ω_i is the eigen frequency of the state $|i\rangle$ at rest, and m is the atomic mass. In the decorrelation approximation [6], the transition rate is generally given as $N_2\langle\Omega\rangle\langle W\rangle$, where Ω is the two-photon Rabi frequency composed of the pump beam and the scattered light in the end-fire mode, W is the single-atom coherence, and the brackets represent a volume average. In the presence of the pump beam, both Ω and W are exponentially amplified in pairs, whereas only W is deposited in the atomic cloud just after the pump beam is turned off. This coherence then begins to decrease according to the first-order correlation function $W(t) = \int dp \Psi_1^*(p + \hbar q)\Psi_2(p)e^{iqpt/m}$, which represents an overlap of two atomic wave packets in real space [14]. Therefore, for higher temperatures, the overlap time decreases with their extents, i.e., the thermal de Broglie length.

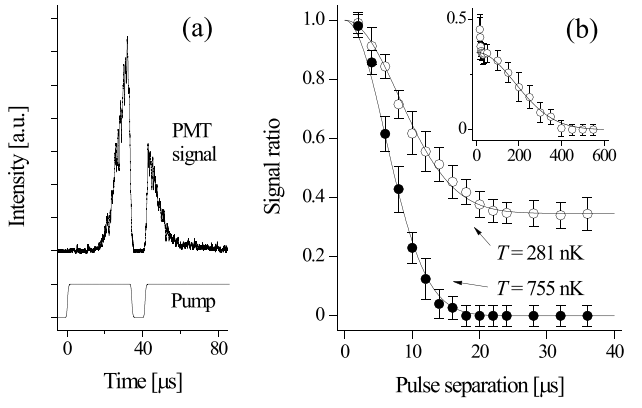

FIG. 3. (a) Scheme of superradiant pump-probe spectroscopy. Lower trace is a timing sequence of the pump beam and upper one is an obtained PMT signal. (b) Decreased fraction of the second peak vs pulse separation. Open and closed circles correspond to a bimodal cloud of $T = 281$ nK and a pure thermal gas of $T = 755$ nK, respectively. Solid lines are fitting curves using a Gaussian function with a constant offset. A decay of the residual offset for $T = 281$ nK is shown in the inset.

Once the pump beam is turned on again, the superradiant pulse is immediately recovered to the level proportional to $|\langle W(t)\rangle|$. Assuming Maxwell-Boltzmann distribution at the same temperature T for $\phi_1(p)$ and $\phi_2(p)$, we obtain

$$|\langle W(t)\rangle| = \exp\left(-\frac{t^2}{\tau_c^2}\right), \tag{1}$$

where τ_c is the e^{-1}-coherence time given as

$$\tau_c = \frac{1}{2k\bar{v}}. \tag{2}$$

Here, $\bar{v} = \sqrt{k_B T/m}$ is the root-mean-square velocity of the atoms. Evidently, the time scale of the decay $\sim 1/(k\bar{v})$ is determined by the Doppler width [8,9].

The decreased fraction of the second superradiant pulse is plotted versus the pump-pulse separation in Fig. 3(b). Open and closed circles represent the data taken from a partially condensed cloud of $T = 281$ nK and a pure thermal gas of $T = 755$ nK, respectively. For the thermal gas, one can clearly see the Gaussian decay as predicted by Eq. (1). Even below T_c, the initial decay is also fitted with a Gaussian curve well, but it no longer drops to zero. This is because the condensate component displays a much longer coherence time than that of the thermal gas. The residual offset is thus a clear signature of the phase transition [15,16].

Figure 4 summarizes the temperature dependence of τ_c. Filled circles are the experimental result obtained from the thermal component, and the solid line is a theoretical prediction given by Eq. (2). We can find their quantitative agreement, which proves the Doppler-width-limited coherence time for thermal-gas SLS.

It is worth emphasizing that the present scheme also allows us to study coherence properties of the condensate component. This is accomplished by monitoring the slow decay of the residual offset, as shown in the inset of Fig. 3(b). We found that the decay shape was also well

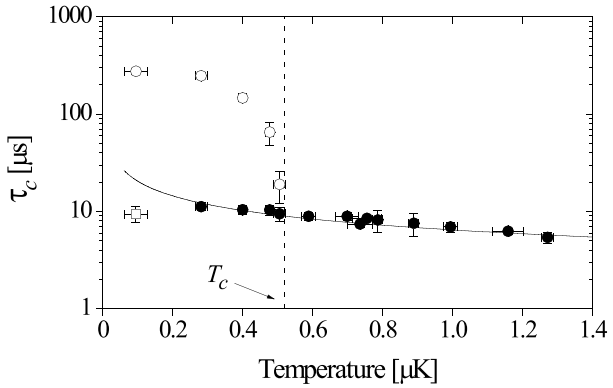

FIG. 4. Coherence time τ_c vs atomic temperature. Open and closed circles correspond to the slow and the fast decay, respectively. Solid line is a theoretical prediction given by Eq. (2). Open square represents the coherence time of a trapped condensate.

fitted with a Gaussian function, but its time scale was about 30 times longer than that of the initial decay. This long-lived coherence steeply built up below T_c (open circles in Fig. 4), and the fast decay disappeared for the pure condensate. The measured τ_c for the pure condensate is 280(20) μs, corresponding to the stimulated Raman spectrum of the full width at half maximum 1.9(1) kHz. This is about three times wider than the finite-sized limit estimated to be $\sim$600 Hz [17], possibly owing to the mean-field expansion during the interval of pump-beam pulses [18]. However, by the grace of the slow recoil velocity of Rb atoms, it is still 2.5 times narrower than the linewidth of the sodium experiment [1].

For comparison, we also measured the coherence time of a ''trapped'' condensate (open square in Fig. 4). The obtained value $\tau_c = 9.6(8)$ μs is comparable with the result in Ref. [2] and demonstrates drastic improvement of the coherence time in the absence of the inhomogeneous magnetic field.

Let us mention that, for sodium atoms, the Doppler width is 2.6 times larger than that of Rb atoms at the same temperature so that thermal-gas SLS is somewhat unfavorable to be carried out. This is presumably the reason for which the thermal-gas SLS of sodium atoms was not observed in the previous experiment [1,9].

In summary, superradiant Raman scattering from non-condensed, thermal rubidium vapors was studied using real-time detection of scattered light pulses and pump-probe measurement of atomic coherence. We were able to characterize various properties, statistical-state-independent gain, conservation of momentum width of the atoms in the amplification process, the Doppler-width-limited coherence time, and sudden occurrence of the long-lived coherence below the transition temperature. This technique is thus a useful tool for the study of coherent atom optics and offers an alternative way to monitor the phase transition. Finally, the present work implies that the superradiant light scattering even in much hotter systems is still possible if enough gain is provided. Accordingly, similar demonstration may be realizable for a more generalized, large variety of samples, including atomic vapors at room temperature, liquids, and solids.

This work was supported by the Grants in Aid for Scientific Research from MEXT, CREST of JST, the Mitsubishi Foundation, and the Matsuo Foundation.

*Electronic address: yutaka@phys.c.u-tokyo.ac.jp

[1] S. Inouye, A. P. Chikkatur, D. M. Stamper-Kurn, J. Stenger, D. E. Pritchard, and W. Ketterle, Science **285**, 571 (1999).
[2] D. Schneble, G. K. Campbell, E. W. Streed, M. Boyd, D. E. Prichard, and W. Ketterle, Phys. Rev. A **69**, 041601(R) (2004).
[3] Y. Yoshikawa, T. Sugiura, Y. Torii, and T. Kuga, Phys. Rev. A **69**, 041603(R) (2004).
[4] D. Schneble, Y. Torii, M. Boyd, E. W. Streed, D. E. Prichard, and W. Ketterle, Science **300**, 475 (2003).
[5] M. G. Moore and P. Meystre, Phys. Rev. Lett. **83**, 5202 (1999).
[6] Ö. E. Müstecaplioglu and L. You, Phys. Rev. A **62**, 063615 (2000).
[7] S. Inouye, T. Pafu, S. Gupta, A. P. Chikkatur, A. Görlitz, D. E. Pritchard, and W. Ketterle, Nature (London) **402**, 641 (1999); M. Kozuma, Y. Suzuki, Y. Torii, T. Sugiura, T. Kuga, E. W. Hagley, and D. Leng, Science **286**, 2309 (1999).
[8] M. G. Moore and P. Meystre, Phys. Rev. Lett. **86**, 4199 (2001).
[9] W. Ketterle and S. Inouye, Phys. Rev. Lett. **86**, 4203 (2001).
[10] For the π polarization, the Raman scattering into the state $|1\rangle$ is the most probable process being preferentially stimulated.
[11] The σ^- component included in a y-polarized light gives the largest rate for the Rayleigh (state-preserving) scattering.
[12] C. K. Law and N. P. Bigelow, Phys. Rev. A **58**, 4791 (1998).
[13] This situation is the same as light pulse propagation in laser medium; see, for example, A. Icsevgi and W. E. Lamb, Jr., Phys. Rev. **185**, 517 (1969).
[14] B. Saubaméa, T. W. Hijmans, S. Kulin, E. Rasel, E. Peik, M. Leduc, and C. Cohen-Tannoudji, Phys. Rev. Lett. **79**, 3146 (1997).
[15] M. Naraschewski and R. J. Glauber, Phys. Rev. A **59**, 4595 (1999).
[16] I. Bloch, T. W. Häncsh, and T. Esslinger, Nature (London) **403**, 166 (2001).
[17] J. Stenger, S. Inouye, A. P. Chikkatur, D. M. Stamper-Kurn, D. E. Pritchard, and W. Ketterle, Phys. Rev. Lett. **82**, 4569 (1999).
[18] E. W. Hagley, L. Deng, M. Kozuma, M. Trippenbach, Y. B. Band, M. Edwards, M. Doery, P. S. Julienne, K. Helmerson, S. L. Rolston, and W. D. Phillips, Phys. Rev. Lett. **83**, 3112 (1999).